

Tapping singular Middle Eastern ultra-sour gas resources combining membrane and absorption systems: Potential for energy intensity reduction

Mohammed Alkatheri^a, Ricardo Grandas^{a,b}, Alberto Betancourt-Torcat^a, Ali Almansoori^{a,*}

^aDepartment of Chemical Engineering, Khalifa University of Science and Technology, The Petroleum Institute, Sas Al Nakhl Campus, Abu Dhabi, P.O. Box 2533, United Arab Emirates.

^bDepartment of Chemical Engineering, Universidad Industrial de Santander, Carrera 27 calle 9, Bucaramanga, Santander, Post Code 678, Colombia.

This Supporting Information file provides additional information on the present study.

1. Operating fundamentals of membrane module in ProMax

In the membrane module, the transport of gases through the dense (nonporous) polymer membranes occurs by a solution-diffusion mechanism. The gas dissolves in the polymer at the membrane high-pressure side, diffuses through the polymer phase, and desorbs or evaporates at the low pressure side. The mass transfer rate depends on the membrane concentration gradient. Moreover, Henry's law is considered to apply (solubility proportional to pressure), and equilibrium is assumed at the membrane interface. It is assumed that the gas-film resistances can be neglected; thus, the partial pressures at the gas-polymer interface are the same as those in the bulk. The flux of gas A can be written using Fick's diffusion law as follows ¹:

$$J_i = -D_i \left(\frac{dC_i}{dz} \right) = D_A \left(\frac{C_{i1} - C_{i2}}{z} \right) \quad (S1)$$

where J_i denotes the flux of gas i , D_i is the diffusion coefficient of the gas, C_{i1} is the equilibrium concentration of the gas in the feed, C_{i2} is the equilibrium concentration of the gas in the low pressure side (permeate). The concentration is related to the partial pressure (P_i) by a solubility coefficient (S), which is the reciprocal of Henry's-law coefficient ¹:

$$C_i = P_i S_i \quad (S2)$$

Using the previous equation to replace the concentration gradient with a pressure gradient results in the following mathematical expression:

$$J_i = \frac{D_i S_i (P_{i1} - P_{i2})}{z} \quad (S3)$$

The product of $D_i S_i$ is the flux per unit pressure gradient, which is called the permeability coefficient (q_i). Since the actual membrane thickness is not always known or specified for commercial membranes, it is customary to use the flux per unit pressure difference (Q_A):

$$J_A = \frac{q_A (P_{A1} - P_{A2})}{z} = Q_A (P_{A1} - P_{A2}) \quad (S4)$$

The permeability ratio between the two gases is identified as the selectivity:

$$\alpha_{AB} = \frac{Q_A}{Q_B} = \frac{D_A S_A}{D_B S_B} \quad (S5)$$

The composition of the permeate and residue (retentate) depend on various factors such as: pressure difference across the membrane, permeability of the different species, feed composition, and feed fraction recovered as permeate. The feed and permeate side pressures are

assumed to be constant. Figure 3 shows details of the membrane module cross flow. The variables X_i and Y_i denote the component i composition in the feed and permeate side, respectively. Additionally, L and V represent the molar flow rate of the feed and permeate, respectively. The membrane module was divided into n completely mixed cross increments (i.e., equal stages) along the module's length, and general mass balances were applied on each element. The feed gas composition (X_i) varies along the membrane fiber axial length, but radial gradients are ignored. However, for the permeate composition at any length it is necessary to distinguish between the average composition (Y_i), and gas composition at the low-pressure side of the skin layer. The latter is also known as local or interface composition ($Y_{i,n}$). The sub-indices $\{n, 0, n_T\}$ denote the incremental, feed, and outlet retentate point, respectively (See Figure 3). The membrane module performance can be estimated using the flux equation for each component as follows:

$$J_i = Q_i(P_1X_i - P_2Y_i) \quad (S6)$$

where P_1 and P_2 are the feed and permeate side pressures, respectively. The local permeate composition at point n ($Y_{i,n}$) is a function of the flux ratio. This can be formulated as follows:

$$Y_{i,n} = \frac{J_{i,n}}{\sum_i J_{i,n}} \quad (S7)$$

where $\sum_i J_{i,n}$ is the sum of local flux of i components at the n^{th} increment.

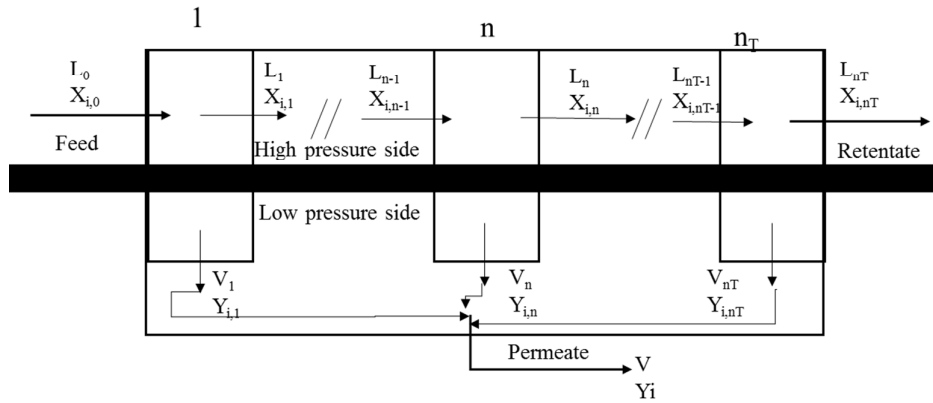


Figure S1. General Layout of the membrane module cross flow.

The composition of component i in the permeate stream along the membrane separator can be expressed as the integrated average of the incremental contribution to V as follows:

$$Y_i = \frac{\sum_{n=1}^{n_T} V_n Y_{i,n}}{V} = \frac{\int Y_{i,n} dV}{V} \quad (S8)$$

where n_T represents the total number of separator increment. The overall and component i material balances for the separator are given as follows:

$$L_0 = L_{nT} + V \quad (S9a)$$

$$L_0 X_{i,0} = L_{nT} X_{i,nT} + V Y_i \quad (S9b)$$

Where V is the summation of the permeate molar flow for all membrane increments (stages).

$$V = \sum_{n=1}^{n_T} V_n \quad (S10)$$

For each stepwise (i.e., stage) of membrane separator incremental length, the following set of equations apply:

$$L_{n-1} = L_n + V_n \quad (\text{S11})$$

$$L_{n-1} X_{i,n-1} = L_n X_{i,n} + V_n Y_{i,n} \quad (\text{S12})$$

Moreover, if the term L_{n-1} in Eq. (12) is replaced by the expression $L_n - V_n$, the following equation is obtained:

$$L_n (X_{i,n-1} - X_{i,n}) = V_n (Y_{i,n} - X_{i,n}) \quad (\text{S13})$$

Equations (7), (10)-(13) are numerically solved to determine the amount of permeate, and its composition for a chosen value of $X_{i,n}$.

Finally, the membrane area required for acid gas separation can be calculated as follows:

$$A = \sum_{n=1}^{n_T} \frac{V_n}{\sum_i J_{i,n}} \quad (\text{S14})$$

To start the calculation algorithm, the permeate stream composition can be assumed to be equal to that of the feed composition. The fluxes are summed to get the total flux and local permeate composition. Successively, the calculation is repeated using the corrected composition (trial-and-error procedure). The procedure is continued for s succession of area increments until the design goal is met¹. This simplified model operates irrespective of equipment geometry. Moreover, the ProMax[®] membrane tool enables performing the separation process based on fixed total area, or solving for the area given desired separation constraints. In particular, for the one-stage membrane the area is determined as a function of the H₂S removal fraction, whereas for the two-stage membrane the H₂S removal fraction is estimated as a function of the membranes' areas. Some hydrocarbon losses occur as the acid gases selectivity is not as optimum as sought. The hydrocarbon losses were calculated for each simulation as they represent a loss opportunity cost in the sweetening process.

2. Stand-alone absorption case study

In the section, a preliminary simulation-based case study was performed to evaluate the performance of different alkanolamines (i.e., MEA, DEA, DGA, and MDEA) for treating ultra-sour natural gas. The performance of the four alkanolamines was evaluated based on the absorption system's total operating costs. The top two performing amine-based systems (in terms of operating costs) were selected for performing hybrid system analysis. The preliminary study simulation results are shown in Table S1. From the table, it can be noticed that the main operating cost for the stand-alone absorption system is the process steam consumption. According to the results, DGA and MDEA are the top two performing solvents for current feed gas conditions because they consider the lowest energy intensity and corresponding utility costs (especially steam) to yield the final sweet gas product. The gas product must meet pipeline specifications at a maximum of 4 ppm of H₂S and 1% mole of CO₂. Consequently, the two solvents were selected to perform a techno-economic analysis on the hybrid schemes.

Table S1. Selected simulation results and annual operating costs for stand-alone absorption systems using different types of alkanolamines.

Alkanolamines	MEA	DEA	MDEA	DGA
System losses				
Stripper hydrocarbon losses (scf/h)	42,300	20,300	15,900	22,500
Flash drum hydrocarbon losses (scf/h)	263,000	130,300	113,500	140,200
Alkanolamines losses (kg/h)	2.72	0.45	0.91	2.27
Energy consumption				
Pump power (kW)	18,600	9,900	6,400	9,300
Solvent cooler (m ³ /h)	16,600	10,000	7,500	9,600
Cooling water flowrate (m ³ /h)	8,800	2,900	1,300	2,100
Steam flowrate (kg/h)	723,900	374,900	260,900	341,600
Annual costs (\$/yr)				
Power	8,048,000	4,289,000	2,766,000	4,013,000
Alkanolamines make-up	9,600	8,200	20,200	65,400
Process steam	152,669,000	79,061,000	55,030,000	72,029,000
Cooling water	2,707,000	1,378,000	940,000	1,247,000
Hydrocarbon losses	12,374,000	6,105,000	5,247,000	6,595,000
Total operating cost	175,807,600	90,841,200	64,003,200	83,949,400

3. Additional results of single membrane stage

3.1 Effect of H₂S removal in the pre-separation step over the membrane area and CH₄ losses

Figure S2 shows the pre-separation step H₂S removal rate effect on membrane area and hydrocarbon losses. As shown in the figure, higher membrane module's H₂S removal levels involve larger areas and hydrocarbon losses. Moreover, it can be observed that the slopes become steeper as a function of the H₂S removal level. This means that H₂S abatement becomes increasingly difficult at higher H₂S removal levels. As a result, it is worth pointing out that relying exclusively on membranes to reduce acid gases content into ppm levels is not feasible. This will require infinite membrane area combined with very large hydrocarbon losses.

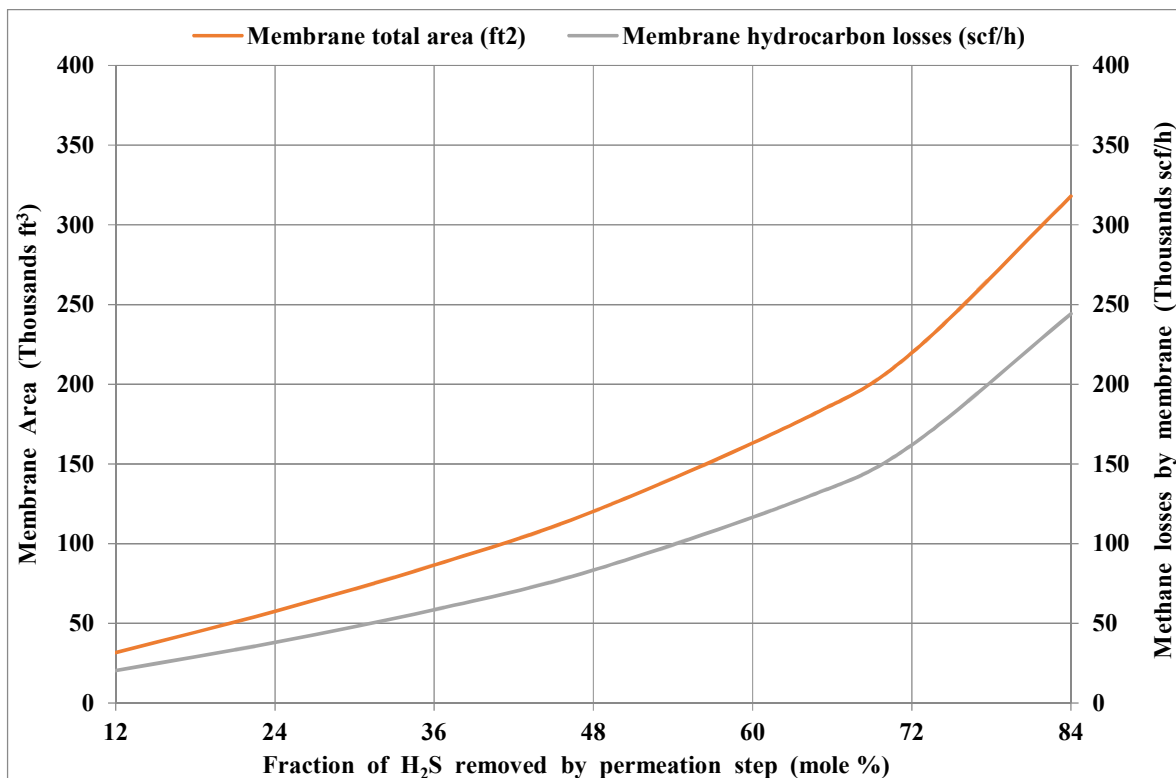


Figure S2 Membrane area and hydrocarbon losses for the one-stage membrane hybrid scheme as a function of the H₂S removed by the membrane module.

Table S2 shows that in the one-stage membrane hybrid scheme (e.g., with MDEA and DGA) the absorber's process steam and cooling water requirements drop as the H₂S fraction in the unit's feed decreases. This directly translates into a lower process energy intensity. Likewise, the recirculation pumps' electricity requirements are directly proportional to the H₂S concentration in the absorber's feed. The total cooling water flowrate (used in condensers and solvent coolers) is considerably higher than the steam. Nonetheless, process steam is significantly more expensive than cooling water (see Table 2).

Table S2. Selected simulation results for the absorption unit in the one-stage membrane hybrid scheme.

Solvent	Variables	% H ₂ S in the absorber's feed			
		22	16	9	4
MDEA	Process steam (kg/h)	218,000	160,000	100,000	56,000
	Condenser cooling water (kg/h)	1,064,000	770,000	496,000	336,000
	Solvent coolers (cooling) water (kg/h)	6,265,000	4,610,000	2,835,000	1,513,000
	Pump electricity (kW)	5,300	3,900	2,500	1,300
	Solvent losses (kg/h)	1.01	1.00	1.01	1.04
	Hydrocarbon losses (scf/h)	106,000	78,000	48,300	26,400
DGA	Process steam (kg/h)	294,000	221,000	143,000	85,000
	Condenser cooling water (kg/h)	1,772,000	1,319,000	830,000	475,000
	Solvent coolers (cooling) water (kg/h)	8,321,000	6,279,000	4,095,000	2,445,000
	Pump electricity (kW)	8,100	6,000	4,100	2,500
	Solvent losses (kg/h)	2.40	2.18	2.05	1.88
	Hydrocarbon losses (scf/h)	140,000	105,000	70,000	42,000

3.2 Effect of H₂S concentration in the absorber's feed over utility costs

Figure S3 displays the total and single utility costs of the one-stage membrane hybrid scheme as a function of the H₂S concentration in the absorber's feed. As shown in the figure, as the amount of H₂S removed by the membrane module increases the utilities demand decrease. This is because the recirculating solvent flowrate (MDEA and DGA) declines in the hybrid systems. It is worth pointing out that the utilities demand are strongly correlated to the concentration of H₂S in the absorber's feed. This is, lower acid gas concentrations in the absorber's feed demand less solvent volumes (recirculation rate) to strip the sulfur content off the valuable hydrocarbon gases (methane). This reduces the electricity requirements in recirculation pumps and solvent coolers. Additionally, as the recirculation rate decreases so does the reboilers' heating load; thus, minimizing steam consumption. Process steam is by far the leading utility cost. Likewise, lower acid gas concentrations in the absorber's feed mean that less acid gases need to be condensed in the regenerator; consequently, reducing cooling water demand.

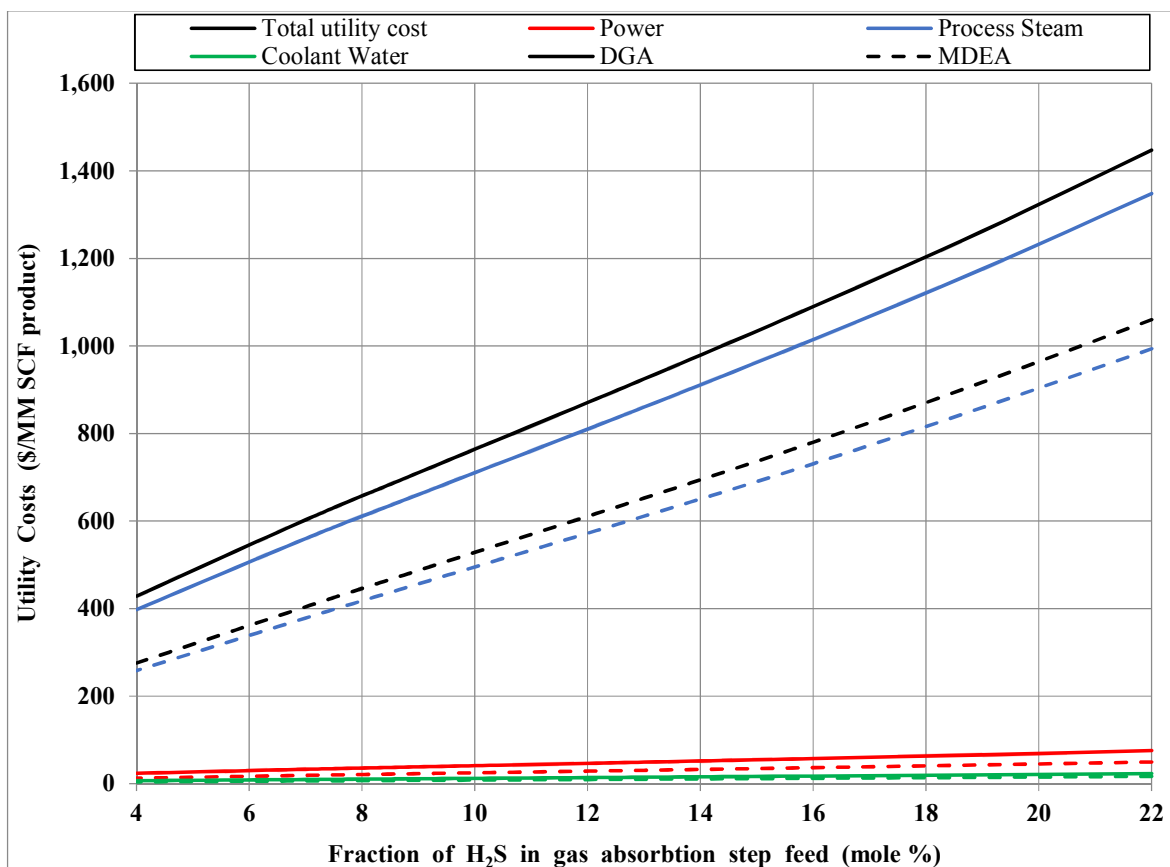


Figure S3 Total and single utility costs for the one-stage membrane hybrid scheme as a function of the H₂S concentration in the gas absorption unit feed (MDEA and DGA).

As shown in Table S2, the H₂S concentration in the absorber's feed has no significant effect on MDEA and DGA losses. On the other hand, the hydrocarbon losses in the absorption unit are inversely proportional to the H₂S fraction removed by the membrane module. Over 90% of the absorber's operating costs are utility expenses. According to the simulation results, when MDEA (e.g., a tertiary and very aggressive alkanolamine to both acid gases) is employed as solvent instead of DGA, the required solvent and utilities demand are lower (see Figure S3).

For any simulation, the thermodynamic package selection is a crucial step. For instance, an appropriate selection of equilibrium properties (i.e., thermodynamic package) is essential for accurate equipment sizing and energy requirement estimations. Acid gases/amines mixture are non-ideal complex systems given the presence of ionic species generated during the chemical reactions between amines (e.g., MDEA, DGA) with acid gases (e.g., CO₂ and H₂S) that take place in the absorber. Nowadays, commercial software have developed powerful tools that can deal with the non-ideal behavior of the system and provide good approximations with respect to real plant data. Particularly, ProMax® offers the “Amine Sweetening” package for natural gas sweetening applications. When this thermodynamic package is selected, the Peng- Robinson Equation of State govern the gas phase calculations, while, liquid phase calculations are estimated using the “Electrolytic ELR” package. Electrolytic ELR was developed by Bryan Research & Engineering to estimate the Gibbs Excess/Activity Coefficient Model. This model calculates the liquid phase activity coefficients based on “Pitzer-Debye-Hückel-PDH” model with noteworthy modifications. The PDH model described in Eq. (1) can be divided in two parts²⁻⁴:

$$\frac{G^{ex}}{RT} = n_w f(I) + \frac{1}{n_w} \sum_{ij} \lambda_{ij}(I) n_i n_j + \frac{1}{n_w^2} \sum_{ijk} \mu_{ijk} n_i n_j n_k \quad (S15)$$

- A) Debye-Hückel term: this term ($f(I)$) is a function of the ionic strength and represents the long-range interactions; while n_w is the amount of solvent per kilogram of water. R is the gas constant, and T is the temperature. On the other hand, n_i, n_j, n_k represent the molality of ions i, j , and k , respectively.
- B) Virial coefficients: λ_{ij} and μ_{ijk} are second and third virial coefficients representing long-range interaction between ions.

An appropriate derivation of Eq. (1) results in an expression for the activity coefficient, which is useful to calculate electrochemical potential. The former combined with the Peng-Robinson equation to estimated fugacity help determining the Vapour-Liquid Equilibrium (VLE) through Henry’s Law. Accordingly, mass and energy balances can be calculated⁵. When an electrolyte dissociates into cations and anions, electrostatic interactions will occur between ion-ion, as well as ion-molecule, and molecule-molecule. To simplify the equations and represent the potential combinations between second and third virial coefficients into more noticeable parameters for a mixture of electrolytes MX-NY with M, N representing cations and X, Y anions; the activity coefficient can be expressed as follows:

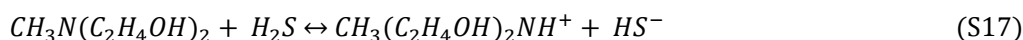
$$\ln(\gamma_{MX}) = z_M^2 f^\phi + m \left\{ \begin{aligned} & (1-y^2) B_{MX^\gamma} + y(\theta_{MN} + \theta_{XY}) + y(1-y) (B_{MY^\phi} + B_{NX^\phi} - 2B_{MX^\phi} + I\theta_{MN} + I\theta_{XY}) \\ & + y^2 (B_{MY^\gamma} - B_{MY^\phi} + B_{NX^\gamma} - B_{NX^\phi} + 2B_{NY^\phi} - B_{NY^\gamma}) \end{aligned} \right\} +$$

$$m^2 \left\{ (1-y)^2 C_{MX^\phi} + y(1-y) (\psi_{MNX} + \psi_{MXY} + C_{MX^\phi} + C_{NX^\phi} + C_{MY^\phi}) + \frac{1}{2} y^2 (\psi_{MNY} + \psi_{NXY} + C_{MY^\phi} + C_{NX^\phi} + C_{NY^\phi}) \right\} \quad (S16)$$

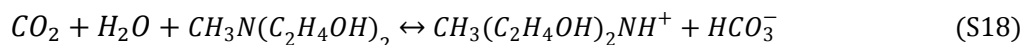
In the above equation, f^ϕ is the derivate of the f term in Eq. (1). In particular, for amines-acid gases systems, parameters B and C define the thermodynamic properties of single-salt solutions. The quantities ψ and θ arise for mixtures and define two-salt systems. The value θ accounts for cation-cation and anion-anion interactions; while ψ takes into account cation-cation-anion and anion-anion-cation interactions^{6,7}.

The advantage of using ProMax is that the interaction parameters obtained from experimental data have been improved using plant data feedback for wide range of conditions and environments like those found in the Middle East Region. Moreover, it is important to notice that reaction kinetics between amines and acid gases in the absorber/stripper are governed by the inlet gas properties as well as the operation conditions of the absorber. The reactions between MDEA and acid gases (i.e., CO₂ and H₂S) can be described as follows:

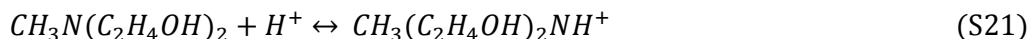
For MDEA and H₂S:



For MDEA and CO₂:



Furthermore, the latter reaction (4) follows three steps. First, a hydrolysis reaction between CO₂ and H₂O (5) which forms carbonic acid that further dissociates into bicarbonate (6). The mechanism concludes with an acid basic reaction that results in a protonated amine (7). Kinetically, the slow rate of reaction (6) controls the whole reaction system^{8,9}.



ProMax® also considers the CO₂-amine or CO₂-carbamate kinetics. The TSWEET Kinetics model, also developed by Bryan Research & Engineering, simultaneously calculates the distillation/absorption and chemical reaction to account for the slow rate of reaction in (6). This rated-based model allows the estimation of the amount of CO₂ removed according to column design and inlet conditions. In TSWEET, the time used in the calculations is the product of the residence time and the real/ideal stage ratio. The residence time can be defined by the user for a preferably H₂S removal¹⁰ or calculated when the flooding and system factor are specified.

Other considerations include the Ishii-Otto algorithms use for the stripper calculations¹¹, and equilibrium solubility modeled through Kent-Eisenberg¹².

5 System Factor

The system factor also known as foaming factor accounts for the tendency of the system to foam. A system factor equals to 1 represents a non-foaming system while very low values indicate a higher foaming tendency. For amines, a system factor of 0.8 can be used for the initial tray and column sizing as most of clean amines does not foam. In gas sweetening applications¹³, the degradation of products and corrosion inhibitors are the main factors affecting the foaming tendency of the system, thus; this can translate into system factor values differing from 1¹⁴.

References

1. McCabe, W. L.; Smith, J. C.; Harriott, P., *Unit Operations of Chemical Engineering*. 5th ed.; McGraw-Hill International Editions: Singapore, 1993.

2. Pitzer, K. S.; Kim, J. J., Thermodynamics of electrolytes. IV. Activity and osmotic coefficients for mixed electrolytes. *Journal of the American Chemical Society* **1974**, 96, (18), 5701-5707.
3. Xu, G.-W.; Zhang, C.-F.; Qin, S.-J.; Gao, W.-H.; Liu, H.-B., Gas-Liquid Equilibrium in a CO₂-MDEA-H₂O System and the Effect of Piperazine on It. *Industrial & Engineering Chemistry Research* **1998**, 37, (4), 1473-1477.
4. Vahidi, M.; Matin, N. S.; Goharrokhi, M.; Jenab, M. H.; Abdi, M. A.; Najibi, S. H., Correlation of CO₂ solubility in N-methyldiethanolamine+piperazine aqueous solutions using extended Debye-Hückel model. *The Journal of Chemical Thermodynamics* **2009**, 41, (11), 1272-1278.
5. Deshmukh, R. D.; Mather, A. E., A mathematical model for equilibrium solubility of hydrogen sulfide and carbon dioxide in aqueous alkanolamine solutions. *Chemical Engineering Science* **1981**, 36, (2), 355-362.
6. Pitzer, K. S., Thermodynamics of electrolytes. I. Theoretical basis and general equations. *The Journal of Physical Chemistry* **1973**, 77, (2), 268-277.
7. Alhseinat, E.; Mota-Martinez, M.; Peters, C.; Banat, F., Incorporating Pitzer equations in a new thermodynamic model for the prediction of acid gases solubility in aqueous alkanolamine solutions. *Journal of Natural Gas Science and Engineering* **2014**, 20, 241-249.
8. Feyzi, V.; Beheshti, M.; Gharibi Kharaji, A., Exergy analysis: A CO₂ removal plant using a-MDEA as the solvent. *Energy* **2017**, 118, 77-84.
9. Dara, S.; Berrouk, A. S., Computer-based optimization of acid gas removal unit using modified CO₂ absorption kinetic models. *International Journal of Greenhouse Gas Control* **2017**, 59, 172-183.
10. Dara, S.; Berrouk, A. S., Effects of residence time on selective absorption of hydrogen sulphide using methyldiethanolamine. *International Journal of Process Systems Engineering* **2014**, 2, (3), 260-272.
11. Paunovic, R. N.; Janković, M. R.; Škrbić, B. D., An extended ishii-otto algorithm for multistage multicomponent separation calculation with stage efficiencies included. *Computers & Chemical Engineering* **1984**, 8, (3), 249-251.
12. Kent, R. L.; Elsenberg, B., BETTER DATA FOR AMINE TREATING. *Hydrocarbon Processing* **1976**, 55, (2), 87-90.
13. Foo, D., *Chemical Engineering Process Simulation*. Elsevier Science & Technology Books: 2017.
14. Alhseinat, E.; Pal, P.; Keewan, M.; Banat, F., Foaming study combined with physical characterization of aqueous MDEA gas sweetening solutions. *Journal of Natural Gas Science and Engineering* **2014**, 17, 49-57.